

K. Tsutsumi
K. Mizoe
K. Chubachi

Adsorption characteristics and surface free energy of $\text{AlPO}_4\text{-5}$

Received: 21 May 1998
Accepted: 28 July 1998

K. Tsutsumi (✉) · K. Mizoe · K. Chubachi
Toyohashi University of Technology,
Tempaku-cho, Toyohashi 441-8580, Japan
e-mail: tsutsumi@tutms.tut.ac.jp
Tel.: +81-532-470111
Fax: +81-532-475460

Abstract The micropores and surface characteristics of aluminophosphate-type zeolite, $\text{AlPO}_4\text{-5}$, were analyzed by examining the adsorption behavior of water and other adsorbates. Water adsorption on $\text{AlPO}_4\text{-5}$ occurred on both structural defects and nonpolar surfaces. Adsorption on structural defects, accompanied by high heats of adsorption, is attributed to adsorption to surface hydroxyls. Water adsorption increased steeply at a certain relative pressure depending on the adsorption temperature, and this was considered attributable to capillary condensation. The contact angle of water on $\text{AlPO}_4\text{-5}$ micropore surfaces can be determined quantitatively by applying the Kel-

vin equation. The surface free energy of $\text{AlPO}_4\text{-5}$ calculated on the basis of the contact angle was revealed to be about 120 mJ/m^2 , in agreement with accepted values of the dispersion component of the surface free energy of metal oxides. Adsorption heat values of adsorbates with different polarities indicate that the $\text{AlPO}_4\text{-5}$ surface is essentially nonpolar and interacts only with dispersion interaction. In the case of *n*-hexane the contact angle was assumed to be zero, showing high affinity with the result of enhanced adsorption due to pore filling.

Key words Adsorption – Surface free energy – $\text{AlPO}_4\text{-5}$ – Contact angle – Kelvin equation

Introduction

Porous aluminophosphates (AlPO_4) have been known to behave as specific adsorbents as well as catalysts by Si or Ti substitution in analogy to porous aluminosilicate zeolites [1–7]. In particular, because synthesis of aluminophosphates with large ring structures has been achieved, aluminophosphate zeolites are of great interest as the specific reaction space with nanometer size [8, 9].

The elementary unit of AlPO_4 consists of oxygen tetrahedra with Al or P as central atoms, which link alternately forming a three-dimensional framework [10]. The unit cell of $\text{AlPO}_4\text{-5}$ used in this study can be represented as $(\text{AlO}_2)_{12}(\text{PO}_2)_{12}$ with hexagonal symmetry with $a = 1.372$ and $c = 0.847 \text{ nm}$. A one-dimensional channel exists in the framework structure along

the *c*-axis consisting of 4-, 6- and 12-oxygen rings [11]. Since an equal number of $(\text{AlO}_2)^-$ and $(\text{PO}_2)^+$ exist in the framework of ideal $\text{AlPO}_4\text{-5}$ zeolites, no exchangeable cation is present.

Considering that the hydrophilicity of zeolites originates from the coexistence of cations and framework anion sites forming an electrostatic field, ideal aluminophosphates should be hydrophobic. However, aluminophosphates have often been observed to be hydrophilic to some extent: this may be explained either by the difference in the electronegativity of Al and P atoms [12, 13] or by the presence of defects in the framework structure [14].

In this study, adsorption characteristics and the surface free energy of $\text{AlPO}_4\text{-5}$ were analyzed by measurements of heats of adsorption and adsorption isotherms of water, argon, nitrogen, carbon monoxide,

methane, and *n*-hexane. Infrared spectroscopic and thermal analyses were also carried out in order to investigate adsorption states of water. Adsorption of water on Na-A zeolite was measured for comparison.

Experimental

The sample, $\text{AlPO}_4\text{-5}$, was kindly supplied by Dr. A. W. Chester of Mobil Research and Development Corporation. The chemical analysis given by the supplier is shown in Table 1. Although the molar ratio Al/P differed from unity, the sample had a high crystallinity according to powder X-ray diffraction. Specific surface area and pore volume determined by nitrogen adsorption in the present study are also shown in Table 1. A commercially available sample of Na-A, which is known to be highly hydrophilic, was used for comparison.

Heats of adsorption and adsorption amount were measured using a conduction calorimeter (Tokyo Riko Co. Ltd.) equipped with a volumetric system [15]. The adsorption isotherm of *n*-hexane was determined gravimetrically. Before measurements, weighed samples were set in a cell, heated at a rate of 1 K/min up to 723 K and kept for 5 h under 1 mPa. Infrared spectra of adsorbed water and hydroxyls were taken using an in-situ cell with a JASCO IR-810 spectrometer. Dynamic behavior of adsorbed water was analyzed using differential scanning calorimetry (DSC) (Seiko DSC 200). Water-saturated samples were heated or cooled in a flow of nitrogen at a rate of 10 K/min.

Results

The adsorption isotherms of water on $\text{AlPO}_4\text{-5}$, as shown in Fig. 1, were type V in the BDDT classification at the adsorption temperatures 303 and 318 K. The amount of adsorption in the low-pressure range was low, whereas at a relative pressure of about 0.3 the amount of adsorption increased steeply. Although $\text{AlPO}_4\text{-5}$ has only low hydrophilicity compared with aluminosilicate-type zeolite, it has a certain number of active adsorption sites. This suggests that adsorption is not accomplished in a single process. Aluminosilicate

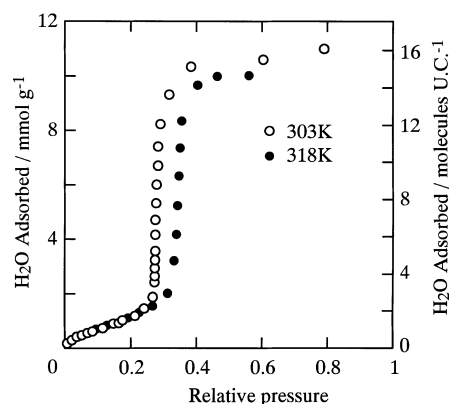


Fig. 1 Adsorption isotherms of water vapor on $\text{AlPO}_4\text{-5}$

zeolite undergoes a chemical interaction with water involving sodium and other cations, and the interaction is also based on hydrogen bonds, with the framework oxygen having a negative charge. The interaction of $\text{AlPO}_4\text{-5}$ with water is considered to be dominated by hydrogen bonds with a certain number of structure forming hydroxyls [14].

Figure 2 shows differential heats of adsorption of water vapor on $\text{AlPO}_4\text{-5}$. Irrespective of the adsorption temperature, the heat of adsorption has values close to the heat of condensation of water ($-\Delta H_L$) throughout the adsorption process, except at the initial stage. This implies that no specific interaction exists between the $\text{AlPO}_4\text{-5}$ surface and water. In the Na-A type studied for comparison (Fig. 3), high adsorption heat, 90 kJ/mol or more, persisted until the amount of adsorption reached some 13 molecules per unit cell (UC), indicating that the Na-A type has high affinity with water molecules because of the presence of a strong electrostatic field.

In $\text{AlPO}_4\text{-5}$ the increasing amount of adsorption (some two molecules per UC) results in a slight increase in adsorption heat. Throughout the adsorption process, however, hydrophobic features tend to dominate. Al-

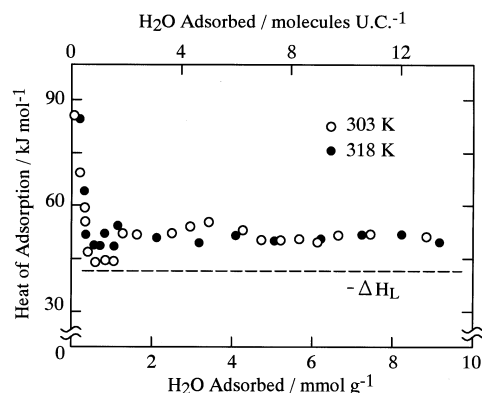


Fig. 2 Differential heats of adsorption of water vapor on $\text{AlPO}_4\text{-5}$

Table 1 Chemical and physical analyses of $\text{AlPO}_4\text{-5}$

Composition	wt %
Al_2O_3	39.4
P_2O_5	50.0
SiO_2	0.08
C	<0.005
Surface area	277 m^2/g
Pore volume	0.16 cm^3/g

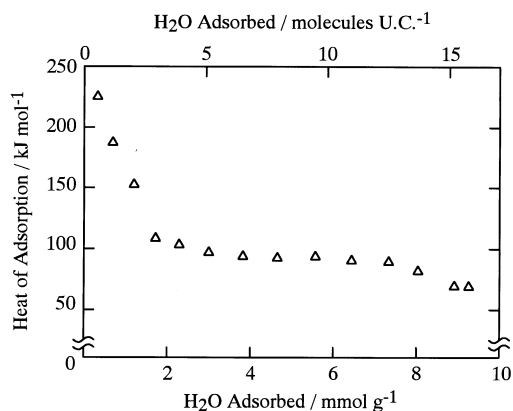


Fig. 3 Differential heats of adsorption of water vapor on Na-A at 303 K

though adsorption time, $t_{1/2}$, until the half-value width of the thermogram accompanying heat generation is long, this is considered attributable to condensation in $\text{AlPO}_4\text{-5}$ micropores. At 0.5 mmol/g adsorption or lower (one molecule per UC or less), however, a high adsorption heat resulted. This may be because structural defects functioned as hydrophilic adsorption sites [14]. The ideal network of $\text{AlPO}_4\text{-5}$ is composed of an Al-O-P linkage and the molar ratio Al/P should be unity. However, one of the Al or P atoms is often lost from the network during synthesis and therefore the T(Al or P)-OH linkage in the framework may appear to retain electrical neutrality. In fact, the molar ratio Al/P of the present sample is 0.91 indicating that mainly P atoms are lost from the network.

Figure 4 presents the results of IR spectra measured in order to locate active sites at the early stage of

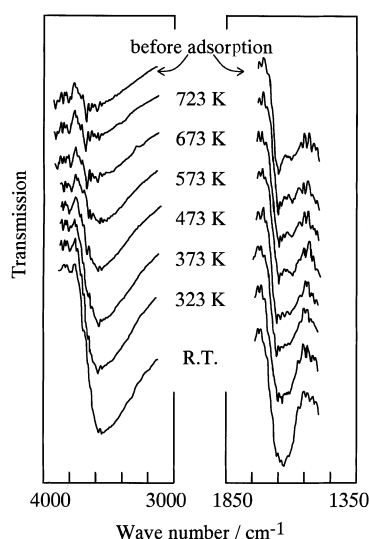


Fig. 4 Infrared spectra of adsorbed water vapor after evacuation

adsorption and to analyze the presence of T-OH groups. After pretreatment under 1 mPa at 723 K, absorption peaks appeared near 3650 cm^{-1} because of the presence of a small number of hydroxyl groups. On the basis of the results of Campelo et al. [2] these hydroxyl groups can be divided into two types: those which resulted from adsorbed water bound to P in the framework and T-OH groups pre-existing therein. Accompanied by adsorption of water (0.5 mmol/g) on the surfaces with these T-OH groups, absorption peaks showing bending and stretching vibrations due to water molecules appeared near 1650 cm^{-1} and 3600 cm^{-1} (bottom spectrum). Evacuating this system under 1 mPa gradually reduced the intensities of two absorption peaks, and at 673 K the intensities reached the intensities of the peaks which had been caused by the surface hydroxyl groups before adsorption. In this case, when adsorption is limited (less than 0.5 mmol/g), water molecules adsorb, though in a very small numbers, to the hydrophilic sites present on the surfaces as T-OH groups by virtue of strong interactions. With regard to active sites attributable to the structural defects of $\text{AlPO}_4\text{-5}$, Moffat [16] revealed the involvement of Lewis and Brønsted acids, and Vasant and Deepak [17] reported measurements of the adsorption of pyridine indicating that a small number of strong Brønsted acid sites was present [17]. Our previous studies also show that the isotopic reactivity of framework oxygen with C^{18}O_2 increased, responding to structural defects [14].

In order to examine the behavior of water molecules adsorbed on $\text{AlPO}_4\text{-5}$, entropy changes, ΔS , caused by adsorption were calculated using Eq. (1).

$$\Delta S = -(q_d + RT)/T - R \ln P_e \quad (1)$$

where q_d was the heat of adsorption and P_e the adsorption equilibrium pressure. As shown in Fig. 5, the Na-A type had a large absolute value ($|\Delta S|$) of ΔS because of surface hydrophilicity, which indicated that the motional freedom of water molecules decreased. The changes were monotonous as a whole, suggesting no

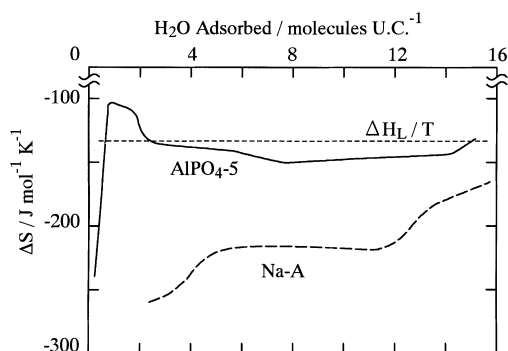


Fig. 5 Differential entropy change by water vapor adsorption

variety of interactions. Nevertheless $|\Delta S|$ continued to decrease, approaching the liquefaction entropy. The fact that the initial adsorption of $\text{AlPO}_4\text{-5}$ has a large value of $|\Delta S|$ corresponds to the interaction with the hydroxyl group sites mentioned above. The $|\Delta S|$ value in the range 2–14 molecules per UC, where the amount of adsorption increased rapidly, was about $150 \text{ J mol}^{-1} \text{ K}^{-1}$. Since this value is close to the liquefaction entropy, it may be due to adsorbed water in micropores behaving like free water.

Discussion

Between the solid surface and an adsorbate, dispersion, repulsive, and polarization forces exist universally, joined by geometrical arrangement, ionization potential, and polarizability of the solid surface and adsorbate [18]. Such a situation occurs when ions and functional groups do not exist on the solid surface or when the solid with such active groups interacts with inactive molecules, such as saturated hydrocarbons. When the adsorbate consists of molecules with permanent dipoles or quadrupoles, the adsorption is joined by field-dipole and field gradient-quadrupole interactions with the surface electrostatic field due to functional groups [19]. One of the present authors, investigating the interaction between various types of zeolite and adsorbate by measuring heats of adsorption, revealed the existence of the surface electrostatic field [20].

In our study the electrostatic field of $\text{AlPO}_4\text{-5}$ was evaluated using the methods of Barrer [21] and Masuda et al. [20]. A plot of initial integral heats of adsorption, for which the interaction between adsorbates seems to be neglected (adsorption at $10 \mu\text{mol/g}$), against the polarizabilities of the adsorbates is shown in Fig. 6. For comparison, the data of the Na-A type reported before [20] is presented in the same diagram. In the Na-A type containing exchange cations (Na^+) in the framework, the use of carbon monoxide or nitrogen with dipolar or

quadrupolar effects causes field-dipole and field gradient-quadrupole interactions, resulting in significant deviation from linear dependency on polarizability. The deviation thus permits the quantitative analysis of the field strength and gradient as well [20]. With $\text{AlPO}_4\text{-5}$ the initial heats of adsorption are low in all adsorbates and simply increase along a nearly linear path irrespective of the type of adsorbates, indicating that the interaction involved is dispersive in the sense that the interaction exists universally. In other words, $\text{AlPO}_4\text{-5}$ possesses virtually nonpolar surfaces on which the contribution of the electrostatic field is almost negligible. This implies that the adsorption of water molecules is due to a nonspecific interaction, excluding the very low adsorption range. The high adsorption heat in this range may possibly be attributed to the lattice defect partially present in crystals. In the ^{18}O isotope-exchange reaction between C^{18}O_2 and the framework oxygen using the same $\text{AlPO}_4\text{-5}$ sample, 2.8 oxygen molecules per UC showed high reactivity [14]. The oxygen molecules with high reactivity were probably produced in T-OH groups that evolved in order to maintain the neutrality of the charge after Al or P was removed from the normal sites. These molecules may cause the IR absorption at 3650 cm^{-1} described earlier in this paper. It is possible that the hydrogen bonds between the T-OH thus developed and water molecules generated high heats of adsorption. After specific adsorption to T-OH sites had finished, free water adsorption to nonpolar surfaces may have occurred.

The rapid increase in the amount of adsorption that followed was probably due to capillary condensation. Hence we applied the Kelvin equation to the $\text{AlPO}_4\text{-5-H}_2\text{O}$ system as follows,

$$\ln(P_e/P_0) = -2\gamma V \cos \theta / rRT \quad (2)$$

where P_e/P_0 is the relative pressure to cause condensation, γ is the surface tension of water, V is the molecular volume, θ is the contact angle of water on $\text{AlPO}_4\text{-5}$, and r is the radius of the micropores. If we let the micropore diameter be 0.73 nm , which is structurally derived, and use relative pressures $P_e/P_0 = 0.27$ and 0.32 , under which the adsorption isotherms rise steeply at adsorption temperatures 303 and 313 K , respectively, the values of $\cos \theta = 0.472$ and 0.449 are obtained.

Generally, the work of adhesion, W , in a solid-liquid system is represented by the Young-Dupr  equation as,

$$W = \gamma_L(1 + \cos \theta) \quad (3)$$

where γ_L is the surface tension of the liquid. Since the surface of $\text{AlPO}_4\text{-5}$ is nonpolar, as previously mentioned, W is expressed by the following equation [22],

$$W = 2(\gamma_L^D \gamma_S)^{1/2}, \quad (4)$$

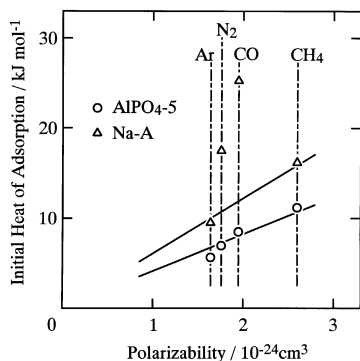


Fig. 6 Change of initial heats of adsorption of various probe gases with polarizability

where γ_L^D represents the dispersion component of the surface tension of the liquid (water in the present study) and γ_S is the $\text{AlPO}_4\text{-5}$ surface free energy, which comprises only the dispersion component. The accepted value of γ_L^D is 21.8 mJ/m² in 72.8 mJ/m² of the surface tension of water at 293 K [23]. From Eqs. (3) and (4), using the values of $\cos \theta$ obtained by the Kelvin equation assuming that the temperature dependency of γ_S , γ_L as well as γ_S^D is negligible in the present temperature range, γ_S can be calculated to be between 115 and 125 mJ/m². This value almost agrees with the γ_S^D values, the dispersion components of solid surface free energy, of SiO_2 , TiO_2 , Al_2O_3 , and similar metal oxides [24]. The latter values were calculated from the free energy of adsorption of *n*-heptane on these solids determined on the basis of the adsorption isotherm. It should be noted that the solid surface free energy from the contact angle obtained by use of the Kelvin equation is comparable with the data obtained from the surface free energy of adsorption. The hypothesis that the surface of $\text{AlPO}_4\text{-5}$ may be nonpolar is also strengthened by this finding.

Where adsorption is nonspecific physical adsorption, as in our present system, the Kelvin equation can be applied to micropores of 1 nm or smaller, suggesting that the principal adsorption process is based on capillary condensation. The sharp rise of the adsorption isotherm indicates that $\text{AlPO}_4\text{-5}$ has a highly homogeneous pore structure.

In water adsorption the amount of saturated adsorption to $\text{AlPO}_4\text{-5}$ reached some two-thirds of that of the Na-A type. Nevertheless these two zeolites greatly differed in heats of adsorption. Thus we examined the evaporation and freezing behavior of adsorbed water by DSC analysis, and observed that the two zeolites showed significant differences when saturated with water as shown in Fig. 7. The hydrophilic Na-A exhibits a broad endothermic peak due to water desorption up to about 550 K, whereas $\text{AlPO}_4\text{-5}$ allows most of the adsorbed

water to evaporate near 373 K. This indicates that the affinity between the $\text{AlPO}_4\text{-5}$ surface and adsorbed water is low and that adsorbed water is considered to behave more like free water when it is evaporating, which is in apparent contrast with water bound to the Na-A zeolite and the Ca-A type [25]. Nevertheless, the evaporation peak persisted beyond 373 K reflecting that the entropy loss due to adsorption was far greater than the liquefaction entropy. This finding is further supported by the observation that no distinctive freezing peak occurred in DSC measurements in the cooling as well as in the heating process between 113 and 313 K. This may indicate that adsorbed water has slightly less freedom of motion than free water and that it does not have full three-dimensional motion for freezing in micropores.

It is known that the solid surface, at which the free energy consists only of the dispersion component, has high affinity with *n*-alkanes. Hence we measured the isotherm of *n*-hexane adsorption on $\text{AlPO}_4\text{-5}$ as shown in Fig. 8. Owing to high affinity, the isotherm turned out to be type I in the BDDT classification. Assuming that the surface free energy consists of a dispersion component ranging from 115 to 125 mJ/m², it can be deduced that the contact angle of liquid *n*-hexane is zero, providing high affinity, thereby enhancing adsorption via pore filling.

Conclusion

The characteristics of water adsorption on $\text{AlPO}_4\text{-5}$ were investigated by measurements of heats of adsorption and adsorption entropy. $\text{AlPO}_4\text{-5}$ has only a small number of relatively strongly hydrophilic sites to which structural defects contribute. Most adsorption is based on capillary condensation. The interaction energy in adsorption is closer in nature to the liquefaction heat of water and no specific interaction with the surface exists. Thus it can be considered that the surface of $\text{AlPO}_4\text{-5}$

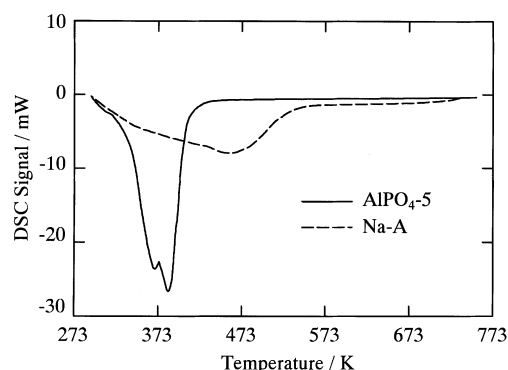


Fig. 7 Differential scanning calorimetry analysis of water evaporation of hydrated $\text{AlPO}_4\text{-5}$ and Na-A

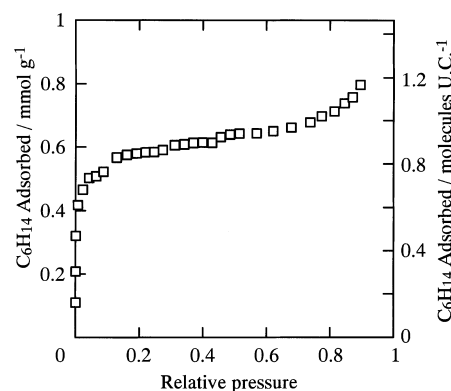


Fig. 8 Adsorption isotherm of hexane vapor on $\text{AlPO}_4\text{-5}$

possesses so few hydrophilic sites that the contribution of the surface electrostatic field can be neglected. The surface free energy of $\text{AlPO}_4\text{-5}$ calculated based on the contact angle was revealed to be about 120 mJ/m^2 , in agreement with the accepted values of dispersion components of the surface free energy of metal oxides.

References

1. Wilson ST, Lok BM, Messina CA, Cannan TR, Flanigan EM (1982) *J Am Chem Soc* 104:1146
2. Campelo JM, Garcia A, Luna D, Marinas JM (1986) *J Catal* 102:299
3. Choudhary VR, Akolekar DB (1987) *J Catal* 103:115
4. Franco MJ, Misfud A, Perez-Pariente J (1995) *Zeolites* 15:117
5. Tuel A (1995) *Zeolites* 15:228
6. Zholobenko V, Garforth A, Clark L, Dwyer J (1995) *Stud Surf Sci Catal* 97:359
7. Masukawa T, Komatsu T, Yashima T (1997) *Zeolites* 18:10
8. Davis ME, Montes C, Hathaway PE, Arhancet JP, Hasha DL, Garces J M (1989) *J Am Chem Soc* 111:3919
9. Davis ME, Saldarriaga C, Montes C, Garces J, Crowder C (1988) *Nature* 331:698
10. Wilson ST, Lok BM, Messina CA, Cannan TR, Flanigan FM (1982) *J Am Chem Soc* 104:1146
11. Wilson ST, Lok BM, Messina CA, Cannan TR, Flanigan FM (1983) *ACS Symp Ser* 218:79
12. Prasad S, Vetrievel R (1994) *J Phys Chem* 98:1579
13. Kitao O, Gubbins KE (1994) *Chem Phys Lett* 227:545
14. Endoh A, Mizoe K, Tsutsumi K, Takaishi T (1989) *J Chem Soc Faraday Trans I* 85:1327
15. Tsutsumi K, Matsushima Y, Matsumoto A (1993) *Langmuir* 9:2665
16. Moffat JB (1985) *J Mol Catal* 30:171
17. Vasant RC, Deepak BA (1987) *J Catal* 103:115
18. Kiselev AV (1965) *Discuss Faraday Soc* 40:205
19. Barrer RM (1972) *J Colloid Interface Sci* 38:195
20. Masuda T, Tsutsumi K, Takahashi H (1980) *J Colloid Interface Sci* 77:238
21. Barrer RM (1966) *J Colloid Interface Sci* 21:415
22. Fowkes FM (1968) *J Colloid Interface Sci* 28:493
23. Fowkes FM (1963) *J Phys Chem* 67:2538
24. Fowkes FM (1964) *Ind Eng Chem* 56:40
25. Stakebake JL (1984) *J Colloid Interface Sci* 99:41